UCRL- 98970
PREPRINT

AUTOIGNITION CHEMISTRY OF N-BUTANE IN A MOTORED ENGINE: A COMPARISON OF EXPERIMENTAL AND MODELING RESULTS

W. J. Pitz
Lawrence Livermore National Laboratory
Livermore, CA

W. R. Leppard
General Motors Research Laboratories
Warren, MI

C. K. Westbrook
Lawrence Livermore National Laboratory
Livermore, CA

This paper was prepared for submittal to
1988 SAE Fuels and Lubricants Meeting
Portland, OR
October 10–13, 1988

June 20, 1988

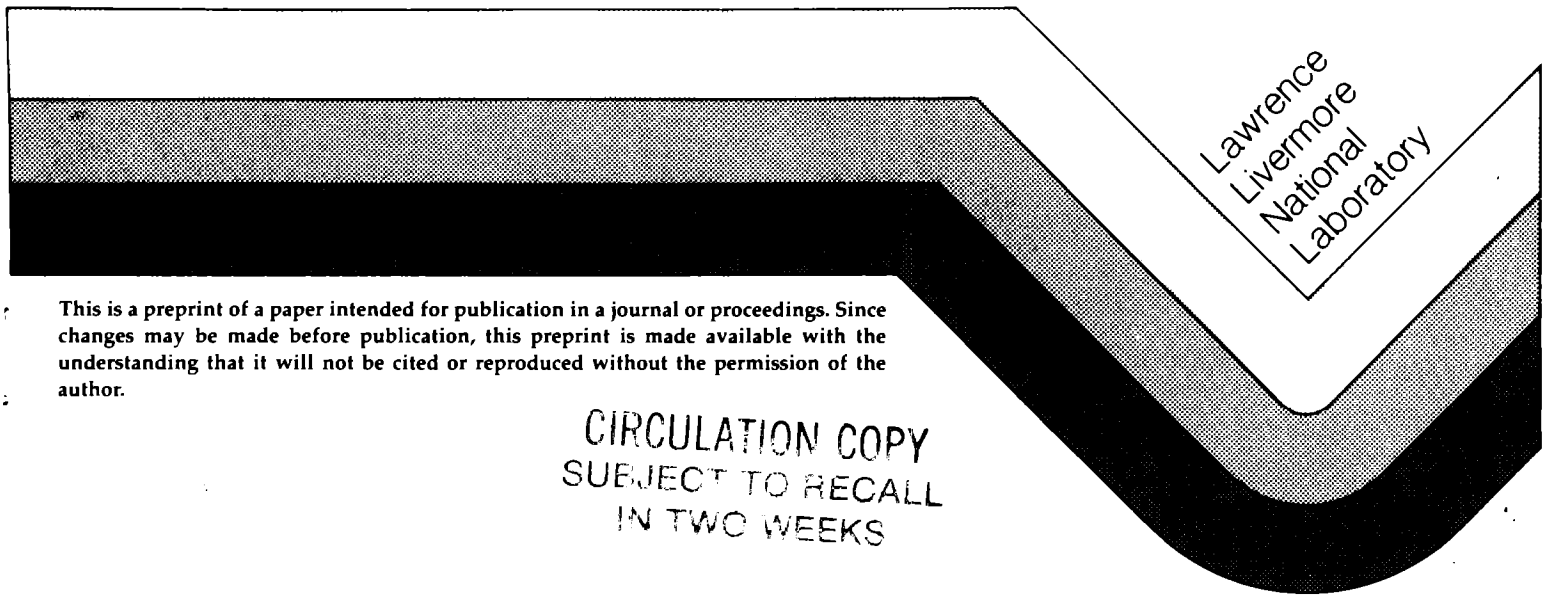

DISCLAIMER

AUTOIGNITION CHEMISTRY OF N-BUTANE IN A MOTORED ENGINE: A COMPARISON OF EXPERIMENTAL AND MODELING RESULTS

W. J. Pitz
Lawrence Livermore National Laboratory, Livermore, California

W. R. Leppard
Fuel and Lubricants Department
General Motors Research Laboratories, Warren, Michigan

C. K. Westbrook
Lawrence Livermore National Laboratory, Livermore, California

submitted to

1988 SAE Fuels and Lubricants Meeting
Portland, Oregon
10-13 October 1988

06/15/1988

Autoignition Chemistry of n-Butane in a Motored Engine: A Comparison of Experimental and Modeling Results

W. J. Pitz
Lawrence Livermore National Laboratory, Livermore, California

W. R. Leppard
Fuel and Lubricants Department
General Motors Research Laboratories, Warren, Michigan

C. K. Westbrook
Lawrence Livermore National Laboratory, Livermore, California

ABSTRACT

A detailed chemical kinetic mechanism was used to simulate the oxidation of n-butane/air mixtures in a motored engine. The modeling results were compared to species measurements obtained from the exhaust of a CFR engine and to measured critical compression ratios. Pressures, temperatures and residence times were considered that are in the range relevant to automotive engine knock. The compression ratio was varied from 6.6 to 15.5 to affect the recycle fraction and the maximum pressure and temperature of the fuel/air mixture. Engine speeds of 600 and 1600 rpm were examined which corresponded to different fuel/air residence times. The relative yields of intermediate species calculated by the model matched the measured yields generally to within a factor of two. The residual fraction derived from the previous engine cycle had a significant impact on the overall reaction rate in the current cycle. The influence of different components in the residual fraction, such as the peroxides, on fuel oxidation chemistry during the engine cycle was investigated.

INTRODUCTION

The theory that autoignition of the end gas is the principal cause of knock has been employed by many researchers over the years [1]. Recently, numerical models have been developed that can model the detailed chemical kinetics that lead to autoignition in the end gas [2-9]. These models allow quantitative comparison between theoretical and experimental species histories in the end gas and comparison of autoignition times. Furthermore, they allow quantitative identification of the principal reactions that control autoignition and knock. Although many of these reactions that control autoignition have been identified by the extensive research performed previously in the area of engine knock, other of these reactions have been thought in prior work to be of minor importance or have been neglected entirely.

In this study, the motored engine technique was employed to follow reactions in a stoichiometric n-butane/air mixture under conditions similar to those found in the end gas of a fired engine. Concentration measurements were made of the stable species in the exhaust gases. The basic premise of the motored engine technique is that the entire fuel/air charge represents the end gas of a fired engine. The maximum temperature and pressure seen by the reactive mixture can be independently controlled by selecting intake temperature, intake pressure, and compression ratio. The residence time of the reactive mixture can be varied by changing the engine speed. This technique allows a close simulation of the temperatures, pressures, and time scales experienced by the end gas in a fired engine. Additionally, the technique allows the study of stoichiometric fuel/air mixtures.

In some other combustion systems, it is difficult to achieve simultaneously all these experimental conditions. For example, the lower

bound in temperature for shock tube experiments is generally around 1100 K which exceeds the temperature normally experienced by the end gas before autoignition. Stirred reactors recirculate the burnt products with the reactants, a process that does not occur in the end gas. The upper bound in temperature for a static reactor is about 750 K so that the important temperature range of 750-900 K is not accessible. In addition, residence times in stirred reactors are considerably longer than in the end gas. Flow reactors normally cannot operate with stoichiometric fuel/air mixtures because of safety considerations.

The motored engine technique has an advantage compared to fired engine experiments because additional cycle-to-cycle variations resulting from fluctuations in the burning rate are absent. Of course, the motored engine technique has its own set of deficiencies. Only the species concentrations in the exhaust gases are usually available. The variation of species concentrations and temperature as a function of time and spatial position in the combustion chamber is generally not available.

There have been a considerable number of important studies that have contributed significantly to the understanding of end-gas chemistry. Green et al. [5,6] have reviewed some of these studies recently, and there are good comprehensive reviews available [e.g. 10-12]. Some studies have addressed specifically the end-gas chemistry for n-butane in engines [2,3,4,6]. Griffiths and co-workers [13,14] examined spontaneous ignition in a rapid compression machine and found that the variation of autoignition time with temperature exhibited a prominent region of negative temperature coefficient behavior. The oxidation of n-butane in static reactors at low and intermediate temperatures has been studied by many investigators, most of whom are cited in References 15 and 16. The mechanism of the high temperature oxidation of n-butane has been

established in experimental and numerical modeling studies in flow reactors, stirred reactors, shock tubes, and flames [17-19].

Some investigators have developed global mechanisms to model end-gas chemistry [20-27]. Najt assessed the "Shell Model" under conditions of threshold knock [25]. His study supported the concept of an ignition temperature for knock [26] and the important role of energy release in the end gas in achieving the ignition temperature.

In the present study, motored engine experiments are described which provide valuable data on the stable intermediate species produced under engine conditions. The experimental results are compared to computed results from a detailed chemical kinetic model for n-butane oxidation. The important chemical kinetic processes identified by the model are discussed.

EXPERIMENTAL AND ANALYTICAL EQUIPMENT AND PROCEDURE

The experimental equipment and method have been discussed in detail [28] and are only summarized here. A Waukesha Cooperative Fuels Research (CFR) engine with several modifications was employed. The cylinder head and piston were modified to allow operation at compression ratios in excess of 15:1. Gaseous n-butane was metered into the intake manifold with a vernier needle valve. The equivalence ratio was continuously monitored with a flame ionization detector sampling from the intake system. Exhaust gas samples were obtained using gas-tight syringes and sampling through a septum located in a slip-stream in the exhaust. To prevent condensation of the high boiling point compounds, the syringes were preheated to 323 K before sampling, and maintained at that temperature until injection into a gas chromatograph for analysis. Three individual gas chromatographs and columns were used to separate all the

intermediate species. This analytical equipment provided a nearly complete spectrum of the concentrations of stable species. Carbon monoxide and carbon dioxide were measured continuously using infrared analyzers. The oxygen concentration in the exhaust was measured continuously with a Scott Model 150A Oxygen Analyzer. Formaldehyde was measured using a technique developed by Lipari and Swarin [29] which employs a dinitrophenylhydrazine derivatizing solution. Hydrogen peroxide was measured using a technique developed by Cullis and Newitt [30].

In-cylinder pressure histories and exhaust gas samples were taken at 600 and 1600 rpm. The intake manifold pressure was maintained at 95 kPa for 600 rpm and 75 kPa for 1600 rpm. The intake manifold temperature was maintained at 440 K. The fuel/air equivalence ratio was 1.00 ± 0.02 for all the measurements. The compression ratio was varied from 6.63 to the critical compression ratios of 8.8 at 600 rpm and 15.5 at 1600 rpm. The repeatability of the species measurements was very good as demonstrated when species concentrations were obtained during experimental runs two years apart, and the concentrations under the same operating conditions agreed to within 10 percent.

NUMERICAL MODEL

The computer modeling analysis was performed using the HCT (Hydrodynamics, Chemistry and Transport) program [31], which solves the coupled chemical kinetics and energy equations. The reaction rate mechanism used in this study has been validated over an extended temperature range. For the low to intermediate temperature range of 550-753 K, the reaction mechanism was developed by comparison of predicted results to experimentally measured results in static reactors [15]. The reaction mechanism has been used to model the autoignition of n-butane in

rapid compression machines with temperatures at the end of compression that range from 700-800 K [32]. At higher temperatures of 1000-1100 K, the reaction mechanism was validated by comparisons to flow reactor data [17]. Additionally, the reaction mechanism has been employed to model fired and motored engine experiments [2,4,6]. For all these comparisons, the fuel was n-butane. The reaction rate mechanism, including forward and reverse rate parameters, is given in Reference 15. Literature values for the rate constants and thermochemistry [33-35] were used whenever possible. When values were unavailable, estimates were made by analogy to similar reactions. For some reactions, we included pressure dependencies from Miller and coworkers [36], and Tsang and Hampson [37]. For reactions whose pressure dependence was not available, we assumed either a high or low pressure limit for the reaction rate.

To achieve sufficient reactivity under the conditions in the motored engine, the rate constants for the reactions

$$C_4H_{10} + RO_2 \rightarrow C_4H_9 + RO_2H \quad (1)$$

$$C_4H_9O_2 \rightleftharpoons C_4H_8O_2H \quad (2)$$

listed in Reference 15 were multiplied by a factor of 1.72 and 4.0 respectively. A similar enhancement of these rate constants was required to achieve sufficient reactivity for n-butane under the conditions of a rapid-compression machine [32]. Under simulated conditions in a motored engine, the overall rate of oxidation of n-butane was very sensitive to the rates of Reactions 1 and 2 as seen in the results of a sensitivity analysis presented later. Reaction 1 represents 22 reactions in the chemical kinetic mechanism since the abstraction of primary and secondary hydrogens by RO_2 to form a primary or secondary butyl radical was considered separately, and R denotes any of 11 different hydrocarbon radicals including the H radical. Reaction 2 represents five possible

alkyl peroxy radical isomerization reactions that are treated explicitly in the mechanism.

Engine cycles at 600 and 1600 rpm were numerically simulated for the entire compression and expansion stroke. We assumed that the temperature of the fuel/air mixture at bottom dead center was 440 K and the pressure was 95 kPa for 600 rpm and 75 kPa for 1600 rpm, which were the conditions in the intake manifold. The HCT program was run with a single computational zone where the volume of the zone varied with crank angle according to the slider crank angle formula [38] (the half stroke to rod ratio was 0.225). The numerical model neglected transport processes in the combustion chamber. Piston blow-by was neglected since measurements showed it to be very small in this CFR engine at these operating conditions. The reactive mixture was assumed to be adiabatic during the engine cycle. This is a good assumption if there is an adiabatic core of combustion chamber gas whose reaction rate is higher than that for other portions of cooler gas, and it controls the rate of reaction in the combustion chamber.

In the motored CFR engine, a significant portion of the gases from one engine cycle are carried over into the next engine cycle and mix with the incoming fuel/air charge. Consequently, the reactions of the fuel/air mixture were followed for an entire compression and expansion cycle, and the final gaseous composition was used as the residual composition for the computation of the next compression-expansion cycle. A series of compression-expansion cycles were calculated until the final concentrations of the gases converged to asymptotic values.

MODELING RESULTS

Modeling calculations were carried out at simulated engine speeds of 600 and 1600 rpm, and at a series of compression ratios. Calculations were performed at each compression ratio at which experimental measurements were made until the compression ratio was sufficiently high to cause autoignition in the model. Figure 1 compares the fuel and alkene concentrations calculated by the model to the measured concentrations in the exhaust gases at 600 rpm. The calculated concentrations of each species at different compression ratios are connected by straight-line segments. When a calculation was performed at a compression ratio of 8.6, autoignition was predicted. Autoignition was observed intermittently in the experiment when the compression ratio was raised above 8.6. As seen in Fig. 1, the alkene concentrations are well predicted at compression ratios of 7.9 and 8.2. The relative amounts of butenes, ethylene and propylene compare well with the experimental measurements. However, the computed levels of 1-butene and 2-butene are reversed compared to the measurements. Additionally, the calculated fuel and alkene concentrations show less sensitivity to a change in compression ratio than the measured concentrations, for compression ratios in the range of 6.6 to 7.4.

All of the measured species concentrations at a compression ratio of 8.2 and an engine speed of 600 rpm are compared to the calculated concentrations in Table I. It is convenient to make a comparison at these experimental conditions since the overall extent of reaction as indicated by the concentration of stable intermediates was approximately the same in the calculation and the experiment. An examination of the calculated and measured concentrations in Table I shows that the major intermediates (formaldehyde, ethylene, acetaldehyde, propylene, 1-butene, 2-butene, and epoxybutane) agree within a factor of two. The predictions for the other

major intermediates (carbon monoxide, carbon dioxide and methanol) are low. The best agreement between measured and calculated concentrations is for the alkenes which are within ±15 percent. The hydrogen peroxide concentration was not shown in Table I since it was measured at the higher compression ratio of 8.3. The predicted concentration of hydrogen peroxide of 2000 ppm at an 8.2 compression ratio is two times higher than the measured concentration of 1000 ppm at 8.3 compression ratio.

Of the stable intermediates, the measured carbon monoxide concentration was the highest. The model predicts a carbon monoxide concentration that is about a factor of 8 too low (Table I). The primary sources for CO in the chemical kinetic mechanism are the reactions:

$$HCO + O_2 \rightarrow CO + HO_2 \quad (3)$$

$$CH_3CO \rightarrow CH_3 + CO \quad (4)$$

The HCO and CH_3CO radicals are derived mainly from the abstraction of an H-atom from formaldehyde and acetaldehyde respectively (the HCO radical also results from the $C_2H_3 + O_2 \rightarrow CH_2O + HCO$ reaction). From Table I, the predicted formaldehyde and acetaldehyde concentrations are low by about a factor of two so that a refinement of the chemical kinetic mechanism to yield the measured amount of these aldehydes would also improve the agreement for the CO concentrations; but not sufficiently to account of a factor of 8 discrepancy.

Modeling calculations were carried out at the higher engine speed of 1600 rpm. At this engine speed, autoignition is predicted by the model at a much lower compression ratio than is observed experimentally. When a modeling calculation was performed at a compression ratio of 11.6, autoignition was predicted. In the experiments, autoignition was observed intermittently at compression ratios exceeding 14.6. The fuel and alkene concentrations for 1600 rpm are shown in Fig. 2. For compression ratios

of 8.94 or less, the predicted ordering of the concentrations of butene, ethylene and propylene is the same ordering observed in the experimental data. However, while the measured alkene concentrations increase moderately over the wide range of compression ratios from 8.9 to 13.7, the predicted alkene concentrations vary moderately with compression ratio only from 7.25 to 8.94, from which point they rise steeply leading to autoignition at a compression ratio of approximately 11.6.

The moderate variation in intermediate concentrations with compression ratio observed in the experimental data in Fig. 2 was also seen in the modeling results at 600 rpm from compression ratios of 6.6 to 7.9. This behavior in the model can be explained by examining the production of radical species as the compression ratio (and thereby the temperature) is increased. The radical species to be examined is the OH radical which controls the oxidation of the fuel at the present conditions. At lower compression ratios where the reactive mixtures are subjected to lower temperatures, the main production path for OH is the sequence [39],

$$R + O_2 \rightleftharpoons RO_2 \rightleftharpoons R'O_2H \rightleftharpoons O_2R'O_2H \rightleftharpoons HO_2R''O_2H \rightarrow XO + \text{carbonyl} + OH + OH \quad (5)$$

where R is a primary or secondary butyl radical, the R' and R'' indicate the removal of an H-atom from R, and X is a smaller hydrocarbon radical. This chemical kinetic route was included in our reaction mechanism [15]. As the compression ratio and temperature increase, it is well known that the contribution of the above path decreases due to the shift of the equilibrium in the $R + O_2 \rightleftharpoons RO_2$ reaction. However, an alternative reaction path increases its production of OH radicals as the temperature is raised,

$$C_4H_{10} + HO_2 \rightarrow C_4H_9 + H_2O_2 \quad (6)$$

$$H_2O_2 + M \rightarrow OH + OH + M \quad (7)$$

$$C_4H_9 + O_2 \rightarrow C_4H_8 + HO_2 \quad (8)$$

and compensates for the decreased contribution from the RO_2 path. (Note that this reaction sequence regenerates the HO_2 radical again to complete the chain cycle.) Therefore, the total OH production from the two reaction paths listed above varies slowly with compression ratio (and temperature) and a "flat region" in the profiles of stable intermediates results.

The model predicts regions where the stable intermediate concentrations are relatively invariant with compression ratio, but these regions occur at lower compression ratios or temperatures than seen in the experimental results. The model does not predict the broad "flat region" in the profiles of the stable intermediates observed experimentally at an engine speed of 1600 rpm (Fig. 2). The position and extent of this "flat region" on a plot of concentrations versus compression ratio is dependent on the value of the equilibrium constant of the $R + O_2 \rightleftharpoons RO_2$ reaction. Calculations were very sensitive to the value of this equilibrium constant, as indicated in the following section. If this equilibrium constant is increased, the model may exhibit an extended "flat region" for an engine speed of 1600 rpm.

At an engine speed of 1600 rpm, the model predicts autoignition at a lower compression ratio (11.6) than is observed experimentally (intermittent autoignition is observed at compression ratios exceeding 14.6). The agreement between the predicted and measured compression ratio at autoignition could be improved at 1600 rpm by considering heat losses from the reactive mixture. The model assumes presently that there is a core of gas in the combustion chamber that is effectively adiabatic. If the model allowed heat losses from this core of gas, the maximum temperature achieved after compression would be lowered and a higher compression ratio would be required for the mixture to autoignite.

Therefore, the inclusion of heat loss in the model raises the predicted compression ratio at autoignition and improves the agreement with the experimental results at 1600 rpm. However, this inclusion of heat loss would also raise the predicted compression ratio at autoignition at 600 rpm and the agreement at this engine speed would worsen.

A sensitivity analysis of the reaction mechanism was performed and the results are presented in Table II. The experimental conditions of an engine speed of 600 rpm and a compression ratio of 8.2 were selected because these conditions were close to the compression ratio (8.6) where the model predicted autoignition. To obtain each sensitivity coefficient in Table II, the forward and reverse reaction rate coefficients of the reaction under consideration were multiplied by a factor of two, and the numerical model was used to calculate new values of the final species concentrations. The sensitivity coefficients are defined by the value of the final fuel concentrations with the original and modified rate coefficient:

$$\text{sensitivity coefficient} = ([\text{fuel}]_{\text{original}} - [\text{fuel}]_{\text{modified}})/[\text{fuel}]_{\text{original}}$$

The amount of fuel consumed indicates the overall extent of reaction that has occurred during the engine cycle. Modeling calculations show that the rapid temperature rise at autoignition occurs just after approximately one half to two thirds of the fuel has been consumed. If a change in a rate constant of a particular reaction causes more of the fuel to be consumed during the engine cycle (a positive sensitivity coefficient), then the reactive mixture has proceeded closer to the point of autoignition. In this case, it can be concluded that this reaction has an accelerating effect on the autoignition process. Autoignition was sufficiently sensitive to the rate coefficient of some reactions that a

factor of two increase caused autoignition to occur (Table II). For reactions which were in partial equilibrium for most of the engine cycle, a factor of two change in their rate coefficient had little effect on the computed results. In these cases, the computed results may be very sensitive to a change in the equilibrium constant of the reaction, and we examined this parameter. Because of the large number of reactions in the mechanism, only reactions which made a significant contribution to the production or consumption of radical species were tested for sensitivity.

The results showed the largest sensitivity to the value of the equilibrium constant of the $R + O_2 \rightleftharpoons RO_2$ reaction (Table II). A factor of two change in the equilibrium constant favoring the formation of RO_2 radicals caused autoignition of the reactive mixture. The equilibrium constants employed for these reactions are based on those measured by Slagle, Gutman and coworkers [40,41] for C_2H_5 and i-C_3H_7.

The next most highly ranked reactions by the sensitivity analysis were the butyl peroxy isomerization reactions followed by the reaction between the fuel and HO_2 radicals. A factor of two increase in these reaction rates also caused autoignition to occur in the modeling calculation. These sensitivity results indicate a significant role of butyl peroxy radical isomerizations in the oxidation of n-butane. They also reaffirm the importance of the reaction between the fuel and HO_2 radicals [3],

$$C_4H_{10} + HO_2 \rightarrow C_4H_9 + H_2O_2 \qquad (9).$$

This reaction path leads to OH radicals when hydrogen peroxide dissociates,

$$H_2O_2 + M \rightarrow OH + OH + M \qquad (10),$$

a reaction which ranked fourth in Table II. The OH radicals produced react primarily with the fuel:

$$C_4H_{10} + OH \rightarrow C_4H_9 + H_2O \quad + \sim 23 \text{ kcal/gmole} \qquad (11)$$

The formation of water is accompanied by a significant amount of energy release which raises the temperature of the reactive mixture and promotes the autoignition process.

Hu and Keck [24] developed a reduced reaction mechanism for the autoignition of hydrocarbons that is very similar to the "Shell Model" [20]. They distinguished between the autoignition characteristics of each fuel that they considered by altering the equilibrium constant for the alkylperoxy radical isomerization reaction, $RO_2 = R'OOH$. We assessed the sensitivity of our chemical kinetic mechanism to this equilibrium constant. The calculated sensitivity was very small (-0.002), which is negligible compared to the other sensitivities in Table II. Our calculations show a considerable sensitivity to the forward rate constant of this reaction (second reaction, Table II), but not to the equilibrium constant which is used in determining the reverse rate constant.

There is considerable discussion in the literature concerning the influence of energy release from low temperature reactions on the autoignition process [6,25,26,28]. The numerical model was used to assess the amount of energy release from chemical reactions prior to autoignition. The temperature history during the engine cycle with chemical reactions was compared to a temperature history with no chemical reactions. The temperature difference between the histories was used as a measure of the energy release from chemical reactions. The temperature histories obtained at a compression ratio of 8.2 and an engine speed of 600 rpm were employed since the calculation for this case exhibited a large extent of reaction (Fig. 1). Calculations showed that the maximum temperature during the cycle increased by 12 K compared to the maximum temperature obtained when the reaction rates were set to zero. This calculated temperature increase of 12 K can be compared to a measured

increase of 18 K at a compression ratio of 8.6 [28]. The calculated temperature increase at a compression ratio of 8.2 was compared to the measured temperature increase at 8.6 because in both cases these compression ratios were the highest that could be examined without autoignition occurring either in the model or the experiment. Considering that reactions have proceeded farther in the experiments at a compression ratio of 8.6 than the model at a compression ratio of 8.2 (as indicated by the level of stable intermediates in Fig. 1), the agreement between the predicted and measured temperature increase is reasonable.

We used the numerical model to assess the importance of energy release from chemical reaction. Prior to the onset of the rapid temperature rise at autoignition, the reaction that makes the largest contribution to energy release is that between the fuel and OH radicals (Reaction 11). We examined the sensitivity of the computed results to the amount of energy released by this reaction. The amount of energy released by this reaction can be increased artificially by altering the enthalpy of formation of water. The enthalpy of formation of water was decreased so that the energy release from Reaction 11 was approximately double the normal value. Since the amount of energy release depends on whether a primary or secondary H-atom is abstracted from the fuel, a value of ΔH^{o}_{f} for H_2O was chosen (-80.8 kcal/gmole) so that the average energy release for Reaction 11 (23 kcal/gmole) was doubled (46 kcal/gmole). The same operating conditions used for the results in Table II were employed for this calculation. The increase in amount of fuel consumed during the engine cycle, as indicated by the previously defined sensitivity coefficient, was used as a gauge of the effect of the increased energy release. The sensitivity coefficient obtained was -0.048 which ranks about tenth on the list in Table II. Consequently, doubling the amount of

energy release that occurs due to the principal reaction releasing heat gave a moderate effect, but not a dominant effect when compared to other reactions having higher sensitivities shown in Table II.

The residual fraction may contain certain molecular components whose presence leads to a greater extent of reaction than would otherwise occur during the engine cycle. We performed a series of calculations to identify these reactive components. Selected species were removed from the residual fraction, and the impact of this removal on the computed results was assessed. We used the change in the amount of fuel consumed during the engine cycle as a measure of the overall effect that a species removal had on the calculated results. When this change is normalized, one obtains the sensitivity coefficient as defined previously. The sensitivity coefficient can be used to rank the effect of removing different components from the residual.

The results are shown in Table III. Removal of peroxides from the residual fraction had the biggest impact on the computed results. Of the various types of peroxides, removal of H_2O_2 had the most significant effect due to its large concentration in the residual fraction. Calculations were sensitive to removal of the alkyl hydroperoxides, but they were present in about 50 times lower concentrations in the residual than hydrogen peroxide. These computed results are consistent with the experimental results of Downs, Walsh and Wheeler [42] who added aldehydes, organic peroxides and hydrogen peroxide to paraffinic fuels in a spark ignition engine. They found that "of all the stable intermediate products of reaction formed in the 'end gas' of the engine prior to knock, organic peroxides (and hydrogen peroxide) are the only ones which have a strong pro-knock action". Removal of aldehydes from the residual fraction had a relatively small impact on the computed results (Table III). This result

suggests that aldehydes do not play as large of role in the chemistry of autoignition, at least under the current conditions, as it has been suggested in the literature [10].

CONCLUSIONS

A chemical kinetic mechanism which covers an extended temperature range was applied to simulate n-butane oxidation in a motored engine. The fuel/air mixture in the motored engine is subjected to conditions similar to those found in the end gas of a spark ignition engine. The predicted levels of major intermediate species generally agreed with the measured levels within a factor of two, except for carbon monoxide, carbon dioxide, and methanol. Further work needs to be performed to identify the discrepancy in the amount of carbon monoxide measured in the experiments and that predicted by the model. The amount of heat release from chemical reactions prior to autoignition calculated by the model was similar to that measured in the experiments at an engine speed of 600 rpm. The compression ratio at which autoignition occurred was well predicted at an engine speed of 600 rpm, but poorly predicted at 1600 rpm. Changes in the chemical kinetic mechanism may be needed to resolve this discrepancy.

The numerical model was used to identify some of the factors controlling autoignition under simulated engine conditions. The autoignition chemistry was most sensitive to the equilibrium constant of the $R + O_2 \rightleftharpoons RO_2$ reaction. The isomerization rate of the alkylperoxy radicals and the reaction between the fuel and HO_2 radicals exhibited the next highest sensitivities. The extent of reaction during the engine cycle calculated by the model was sensitive to the presence of the residual fraction from the previous cycle. Calculations showed that the hydrogen peroxide and the alkyl hydroperoxides in the residual

fraction were responsible for this sensitization. The effect of heat release by low temperature reactions on the progress of the autoignition chemistry was investigated. Under one set of conditions, the heat release from the formation of H_2O (which the model indicated is the primary source of exothermicity prior to high temperature ignition) had a moderate effect on the autoignition process.

ACKNOWLEDGMENTS

The computational modeling portions of this work were supported by U.S. Department of Energy, Office of Energy Utilization Research, Division of Energy Conversion and Utilization Technologies, and were performed under the auspices of the U.S. Department of Energy by the Lawrence Livermore National Laboratory Contract No. W-7405-ENG-48. The experimental portion of this work was performed at General Motors Research Laboratories.

REFERENCES

1. W. Affleck, and A. Fish, "Knock: Flame Acceleration or Spontaneous Ignition?" Combust. Flame, v 12, p 243-252 (1968).

2. Smith, J. R., Green, R. M., Westbrook, C. K., and Pitz, W. J. "An Experimental and Modeling Study of Engine Knock", Twentieth Symposium (International) on Combustion, p. 91, The Combustion Institute, Pittsburgh (1984).

3. Pitz, W.J., and Westbrook, C.K., "Chemical Kinetics of the High Pressure Oxidation of n-Butane and Its Relation to Engine Knock", Combust. Flame, v 63, p 113 (1986).

4. Cernansky, N.P., Green, R.M., Pitz, W.J., and Westbrook, C.K., "Chemistry of Fuel Oxidation Preceding End-Gas Autoignition", Combust. Sci. Technol. v 50, p 3 (1986).

5. Green, R.M., Parker, C.D., Pitz, W.J., and Westbrook, C.K., "The Autoignition of Isobutane in a Knocking Spark Ignition Engine", SAE paper 870169, Detroit, MI, November (1987).

6. Green, R.M., Cernansky, N.P., Pitz, W.J., and Westbrook, C.K., "The Role of Low Temperature Chemistry in the Autoignition of n-Butane", SAE paper 872108, Toronto, November (1987).

7. Leppard, W., "A Detailed Chemical Kinetics Simulation of Engine Knock", Combust. Sci. Tech. v 43, p 1 (1985).

8. Esser, C., Maas, U., and Warnatz, J., Trans. of COMMODIA - International Symposium on Diagnostics and Modeling of Combustion in Reciprocating Engines, Tokyo, Japan, 1985, p. 335.

9. Westbrook, C.K., Warnatz, J., Pitz, W.J., "A Detailed Chemical Kinetic Reaction Mechanism for the Oxidation of Iso-Octane and N-Heptane over an Extended Temperature Range and Its Application to Analysis of Engine Knock", To be presented at the Twenty-Second Symposium (International) on Combustion, Seattle, WA (1988).

10. Pollard, R.T., "Comprehensive Chemical Kinetics", (C.H. Bamford, and C.F.H. Tipper, Eds.), Vol. 17, p. 249, Elsevier, 1977.

11. Griffiths, J.F., "The Fundamentals of Spontaneous Ignition of Gaseous Hydrocarbons and Related Organic Compounds", Adv. Chem. Phys. v 64, p 203 (1986).

12. Lignola, P.G., and Reverchon, E., "Cool Flames", Prog. Energy Combust. Sci. v 13, p 75 (1987).

13. Griffiths, J.F., and Nimmo, W., "Spontaneous Ignition and Engine Knock under Rapid Compression", Combust. Flame, v 60, p 215 (1985).

14. Franck, J., Griffiths, J.F., and Nimmo, W., "The Control of Spontaneous Ignition under Rapid Compression", Twenty-first Symposium (International) on Combustion, p. 447, The Combustion Institute, Pittsburgh (1988).

15. Pitz, W.J., Wilk, R.D., Cernansky, N.P., and Westbrook, C.K., "The Oxidation of n-Butane at Low and Intermediate Temperatures", presented at the Western States Section/The Combustion Institute, Salt Lake City, Utah, March (1988).

16. Wilk, R.D., Cernansky, N.P., Cohen, R.S., "The Transition in the Oxidation Chemistry of n-Butane from Low to Intermediate Temperatures", presented at the Western States Section/The Combustion Institute, paper #85-31, (1985).

17. Pitz, W. J., Westbrook, C. K., Proscia, W. M., and Dryer, F. L., "A Comprehensive Chemical Kinetic Reaction Mechanism for the Oxidation of n-Butane", Twentieth Symposium (International) on Combustion, p. 831, The Combustion Institute, Pittsburgh (1985).

18. Cathonnet, M., Boettner, J.C., and James, H., "Experimental Study and Numerical Modeling of High Temperature Oxidation of Propane and n-Butane", Eighteenth Symposium (International) on Combustion, p. 903, The Combustion Institute, Pittsburgh (1981).

19. Warnatz, J., "The Mechanism of High Temperature Combustion of Propene and Butane", Combust. Sci. Tech., v 34, pp 177-200 (1983).

20. Halstead, M.P., Kirsh, L.J. and Quinn, C.P., "The Autoignition of Hydrocarbon Fuels at High Temperatures and Pressures - Fitting of a Mathematical Model", Combust. Flame v 30, p 45 (1977).

21. Kirsch, L.J., and Quinn, C.P., "Progress Towards a Comprehensive Model of Hydrocarbon Autoignition", J. Chim. Phys. v 82, p 459 (1985).

22. Cox, R.A., and Cole, J.A., "Chemical Aspects of the Autoignition of Hydrocarbon-Air Mixtures", Combust. Flame v 60, p 109 (1985).

23. Morley, C., "A Fundamentally Based Correlation between Alkane Structure and Octane Number", Comb. Sci. Tech., v 55, pp 115-123 (1987).

24. Hu, H.,and Keck, J.C., "Autoignition of Adiabatically Compressed Combustible Gas Mixtures", SAE paper 872110 (1987).

25. Najt, P.M., "Evaluating Threshold Knock with a Semi-Empirical Model -- Initial Results", SAE paper 872149, Toronto, November (1987).

26. Gluckstein, M.E. and Walcutt, C., "End-Gas Temperature-Pressure Histories and their Relation to Knock", SAE Trans. v 69, p 529 (1961).

27. Natarajan, B. and Bracco, F.V., "On Modeling Auto-Ignition in Spark-Ignition Engines", Combust. Flame v 57, p 179 (1984).

28. Leppard, W.R., "The Autoignition Chemistry of n-Butane: An Experimental Study", SAE paper 872150, November (1987).

29. Lipari, F. and Swarin, S.J., "Determination of Formaldehyde and Other Aldehydes in Automobile Exhaust with an Improved 2,4-Dinitrophenyl-hydrazine Method", J. Chromatog., v 247, pp 297-306 (1982).

30. Cullis, C.F. and Newitt, E.J., "The Gaseous Oxidation of Aliphatic Alcohols. I. Ethyl Alcohol: The Products Formed in the Early Stages", Proc. Roy. Soc. Lond., A 237, pp 530-542 (1956).

31. Lund, C.M., "HCT - A General Computer Program for Calculating Time-Dependent Phenomena Involving One-Dimensional Hydrodynamics, Transport, and Detailed Chemical Kinetics", Lawrence Livermore National Laboratory, Livermore, CA, report UCRL-52504 (1978).

32. Westbrook, C.K., Griffiths, J., and Pitz, W.J., manuscript in preparation (1988).

33. "JANAF Thermochemical Tables", U.S. Government Printing Office, Washington, D.C. (1971).

34. Bahn, G.S., "Approximate Thermochemical Tables for Some C-H and C-H-O Species", NASA report NASA-CR-2178 (1973).

35. Benson, S.W., "Thermochemical Kinetics", Wiley, New York, 1976.

36. Glarborg, P., Miller, J.A., and Kee, R.J., "Kinetic Modeling and Sensitivity Analysis of Nitrogen Oxide Formation in Well-Stirred Reactors", Combust. Flame v 65, p 177 (1986).

37. Tsang, W. and Hampson, R.F., "Chemical Kinetic Data Base for Combustion Chemistry. Part 1. Methane and Related Compounds", J. Phys. Chem. Ref. Data v 15, p 1087 (1986).

38. Ferguson, C.R., Green, R.M., and Lucht, R.P., "Unburned Gas Temperatures in an Internal Combustion Engine: II. Heat Release Computations", Combust. Sci. Tech., v 55, pp 63-81 (1987).

39. Benson, S. W., "The Kinetics and Thermochemistry of Chemical Oxidation with Application to Combustion and Flames", Prog. Energy Combust. Sci. v 7, p 125 (1981).

40. Slagle, I.R., Ratajczak, E., Heaven, M.C., Gutman, D. and Wagner, A.F., "Kinetics of Polyatomic Free Radical Produced by Laser Photolysis. 4. Study of the Equilibrium i-C_3H_7 + O_2 = i-$C_3H_7O_2$ between 592 and 692 K", J. Am. Chem. Soc. v 107, p 1838 (1985).

41. Slagle, I.R., Ratajczak, E., and Gutman, D., "Study of the Thermochemistry of the C_2H_5 + O_2 = $C_2H_5O_2$ and t-C_4H_9 + O_2 = t-$C_4H_9O_2$ Reactions and of the Trend of the Alkylperoxy Bond Strengths", J. Phys. Chem. v 90, p 402 (1986).

42. Downs, D., Walsh, A.D., and Wheeler, R.W., "A Study of the Reactions that Lead to 'Knock' in the Spark-Ignition Engine", Phil. Trans. Royal Soc. Lond. A, v 243, pp 463-524, (1951).

FIGURES

Figure 1. Concentration profiles of the fuel n-butane and stable intermediate alkenes as functions of compression ratio (engine speed 600 rpm). The symbols represent experimental data, and the curves represent results of the numerical model.

Figure 2. Concentration profiles of the fuel n-butane and stable intermediate alkenes as functions of compression ratio (engine speed 1600 rpm). The symbols represent experimental data, and the curves represent results of the numerical model.

Table I

Measured and Calculated Species Concentrations
(600 rpm, 8.2 compression ratio)

Species	Concentration (PPM)	
	Measured	Calculated
carbon monoxide	5200	639
carbon dioxide	400	12
methane	73	5
formaldehyde	1816	1060
methanol	662	133
ketene	a	364
ethylene	721	618
acetaldehyde	1867	955
propylene	373	357
propanal	266	111
propenal	266	36
1-butene	1376	1190
2-butene	1103	1290
n-butane	20500	26000
epoxybutane	472	281
2-methyloxetan	a	246
tetrahydrofuran	42	71
oxygen (O_2), [%]	18.9	19.7

[a] not identified

Table II

Reaction Rate Sensitivity
(600 rpm, 8.2 Compression Ratio)

	Reaction			Autoignition Time [ms]	Sensitivity[a] Coefficient
1.	$R+O_2$	→	RO_2	49.2[b]	
2.	RO_2	⇌	$R'OOH$	50.3	
3.	$C_4H_{10}+HO_2$	⇌	$C_4H_9+H_2O_2$	53.6	
4.	H_2O_2+M	⇌	$OH+OH+M$	54.2	
5.	$C_4H_9+O_2$	⇌	$C_4H_8+HO_2$		-0.111
6.	RO_2+HO_2	⇌	$ROOH+O_2$		0.063
7.	HO_2+HO_2	⇌	$H_2O_2+O_2$		0.062
8	$O_2R'OOH$	⇌	$HO_2R''OOH$		0.062
9.	$C_4H_{10}+CH_3O_2$	⇌	$C_4H_9+CH_3O_2H$		0.058
10.	$R'OOH$	⇌	$R'O+OH$		-0.047
11.	$O_2R'OOH$	→	$O_2+R'OOH$		-0.038[b]
12.	$C_4H_{10}+OH$	⇌	$C_4H_9+H_2O$		0.034
13.	$ROOH$	⇌	$RO+OH$		0.030
14.	$s\text{-}C_4H_9$	⇌	$C_3H_6+CH_3$		0.027
15.	$CH_3O_2+CH_3O_2$	⇌	$CH_2O+CH_3OH+O_2$		-0.020

[a] based on fuel concentration at end of cycle.

[b] represents sensitivity to change in equilibrium constant.

Table III

Influence of the Composition of the Residual Fraction on the Overall Extent of Reaction (600 rpm, 8.2 Compression Ratio)

	Component(s) Removed	Sensitivity[a] Coefficient	Mole Fraction in Residual
1.	hydrogen peroxide	-0.059	2.0×10^{-3}
2.	peroxides (excluding hydrogen peroxide)	-0.036	4.0×10^{-5}
	s-butyl hydroperoxide	-0.012	8.9×10^{-6}
	methyl hydroperoxide	-0.007	2.0×10^{-5}
3.	aldehydes	-0.005	2.2×10^{-3}
4.	peroxy radicals (excluding HO_2)	-0.001	2.3×10^{-7}
5.	Other:		
	hydrogen peroxo radical, (HO_2)	-0.001 → 0.0	4.2×10^{-7}
	alkoxy radicals (RO)		3.4×10^{-11}
	hydroxyl radicals (OH)		8.8×10^{-13}
	olefins		3.5×10^{-3}

[a] based on fuel concentration at end of cycle.

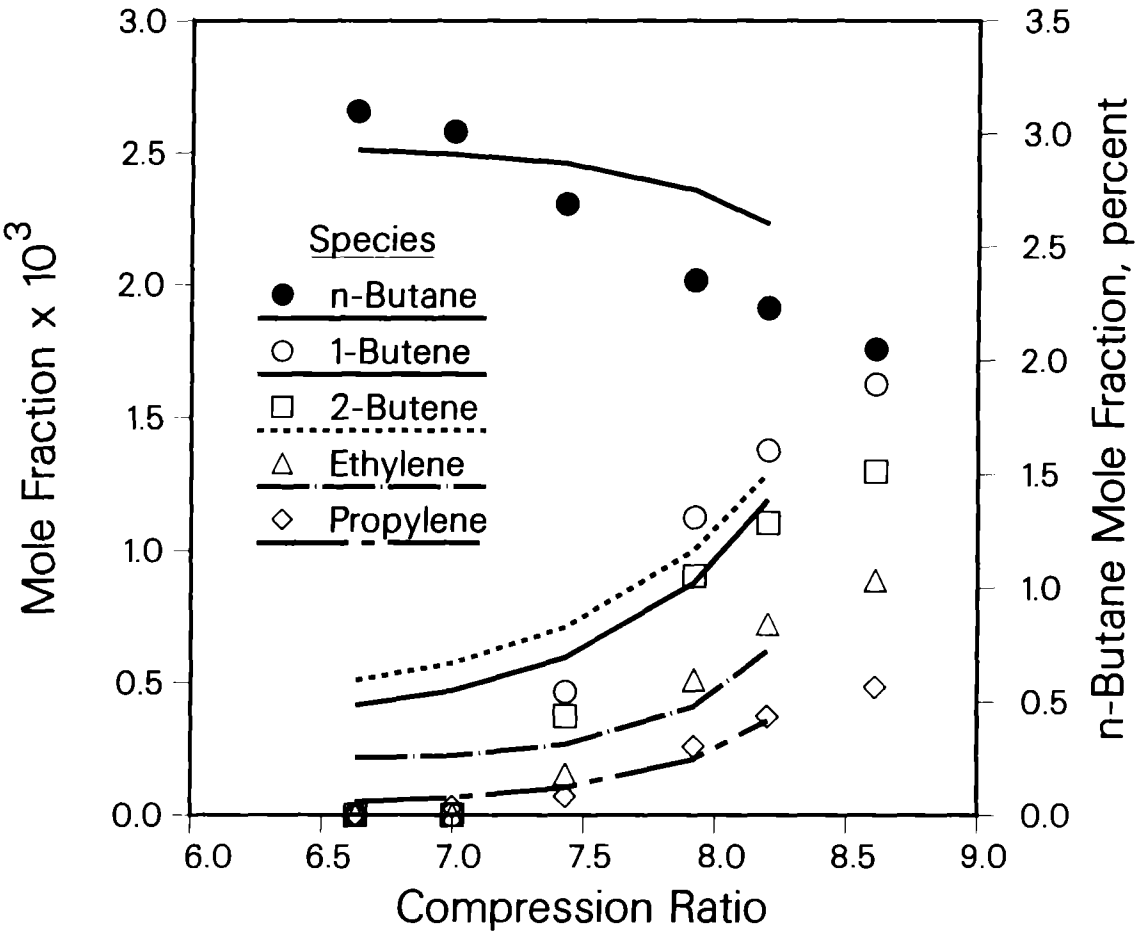

Figure 1. Concentration profiles of the fuel n-butane and stable intermediate alkenes as functions of compression ratio (engine speed 600 rpm). The symbols represent experimental data, and the curves represent results of the numerical model.

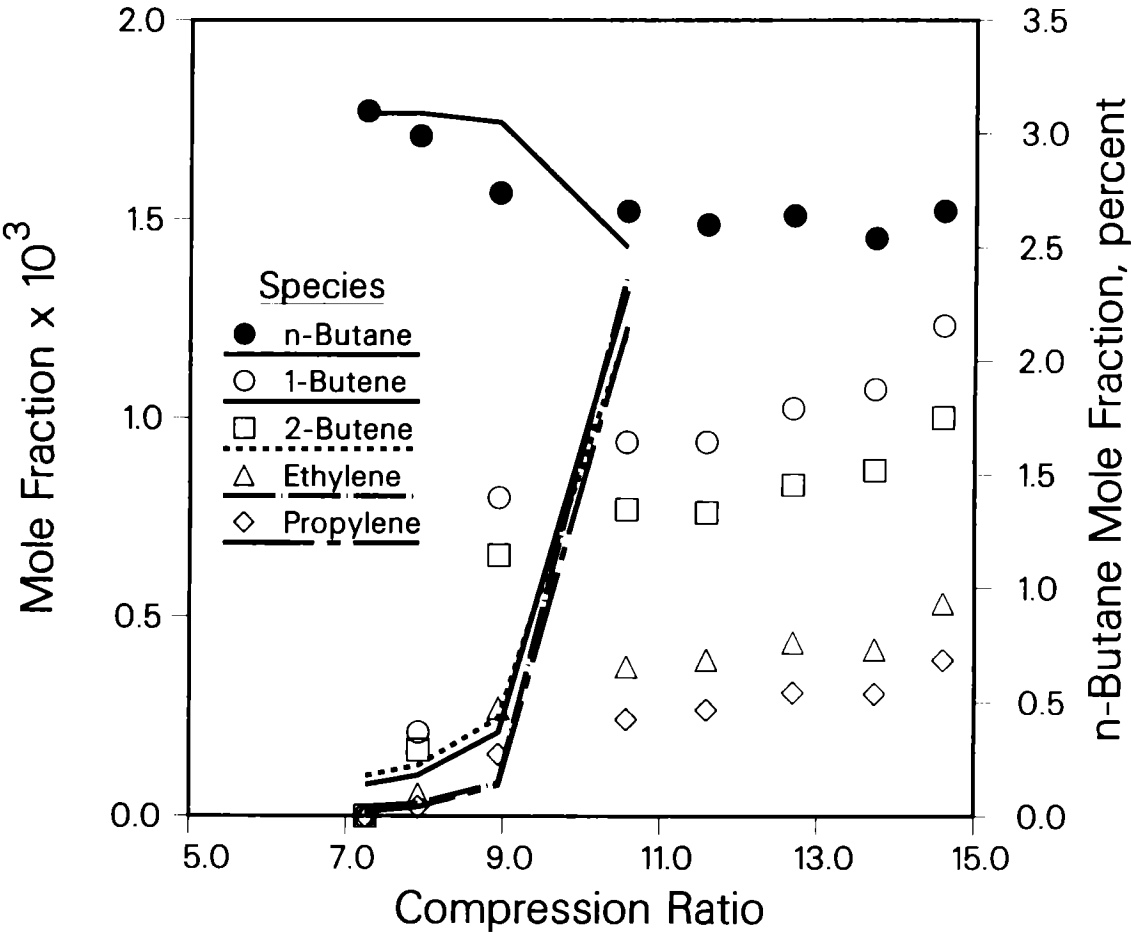

Figure 2. Concentration profiles of the fuel n-butane and stable intermediate alkenes as functions of compression ratio (engine speed 1600 rpm). The symbols represent experimental data, and the curves represent results of the numerical model.